ELSEVIER

Journal of Nuclear Materials 313–316 (2003) 32–41

journal of nuclear materials

www.elsevier.com/locate/jnucmat

# PSI issues at plasma facing surfaces of blankets in fusion reactors

Y. Ueda [a,*], K. Tobita [b], Y. Katoh [c]

[a] *Electronic Information System and Energy Engineering, Graduate School of Engineering, Osaka University, 2-1 Yamadaoka, Suita, Osaka 565-0871, Japan*

[b] *Japan Atomic Energy Research Institute, Naka-machi, Naka-gun Ibaraki, 311-0193, Japan*

[c] *Institute of Advanced Energy, Kyoto University, Uji, Kyoto 611-0011, Japan*

**Abstract**

Important PSI issues for the first wall of blankets in fusion reactors are reviewed. Present understandings and remaining issues for particle loads (fast neutral, thermal ions, and energetic alpha particle ripple losses), and evaluation of low-activation structural materials (RAF, V-alloys, and $SiC_f/SiC$) and tungsten as first-wall armor (including the effect on tritium breeding ratio of blankets) are explained. If the characteristics of particle load to the first-wall evaluated for ITER-FEAT is similar to DEMO and future reactors, erosion rates of the blanket first-wall made by low-activation materials are not acceptable considering their thickness. For this case, armor materials such as W or some protection methods such as in-situ coatings of low $Z$ materials could be needed. Blistering and H/He embrittlement are also important issues to consider. Possible effects of the first wall on core plasma performance are briefly discussed in terms of hydrogen isotope recycling and reflection of synchrotron radiation.


*PACS:* 52.40.H

*Keywords:* Blanket first wall; First wall particle load; Low activation materials; Sputtering erosion; Tritium breeding ratio; Blistering

## 1. Introduction

In DEMO and future commercial reactors, unlike present tokamak devices and next-step devices such as ITER-FEAT, steady-state operation is required, leading to very high particle fluence of roughly $10^{28}/m^2$ (based on ITER-FEAT calculation [1]) onto plasma facing surfaces of blankets. These particle loads consist mainly of DT charge exchange neutrals and ions (high energy alpha particles (ripple loss) could impinge locally). Under the very high heat and particle loads as well as neutron loads, blanket first walls must not be eroded completely or seriously damaged during operation periods of blankets (typically 3 years).

First walls of future fusion reactors are not simple boundary between plasmas and vessels, but they are outer surfaces of blankets, which have several important functions, such as tritium generation and recovery, radiation shielding and energy conversion. Therefore, optimization of the first wall must be done from the viewpoints of not only plasma performance such as impurity control and hydrogen recycling but also blanket functions and its reliability.

Liquid surface concepts are also being studied [2–4] because of some attractive features. Replenishment can counteract erosion, neutron damage (for thick liquid wall), and aid in recovery from off-normal event. Liquid surface in principle could exclude adjusting the heat removal and particle retention/release characteristics of plasma-facing components. Remaining issues to be investigated include MHD effects and evaluation of effects on plasma performance. The details are described in Refs. [2,3] and are not discussed in this paper.

* Corresponding author. Tel./fax: +81-6 6879 7236.
*E-mail address:* yueda@eie.eng.osaka-u.ac.jp (Y. Ueda).

0022-3115/03/$ - see front matter 
PII: S0022-3115(02)01329-6

Off-normal events such as disruption and vertical displacement events (VDEs) [5] are also matters of concern for protecting plasma-facing surfaces against very high heat load and very high electromagnetic force on in-vessel components. Designing fusion reactors to withstand these off-normal events represent a challenging task. Therefore, elimination or sufficient mitigation of the off-normal events is a necessary condition for practical fusion reactors. Suppression and mitigation of these abnormal events are described in Ref. [6]. These topics are not also discussed in this paper.

In this review, particle loads to the first wall in fusion reactors are discussed, especially estimation of fast neutrals and alpha particle ripple losses, and its effects on erosion and surface modification of low activation materials (RAF, V-alloy, and SiC) and tungsten. In addition, effects of the first wall on tritium breeding ratio (TBR) of blankets and core plasma performance are also briefly discussed.

## 2. Heat and particle load to first wall

### 2.1. General

In fusion reactors, the first wall of blankets is subjected to surface heat load due to radiation and alpha particle ripple losses and bulk heating due to neutrons. Although total alpha particle ripple loss power is very low, its contribution to heat flux is not negligible due to its localized feature. Particle fluxes such as fast neutrals and thermal ions play an important role in erosion and modification of the first wall, but its contribution to heat flux is small. Heat flux to the first wall by fusion neutrons is not negligible in power reactors. For example, under the 5 MW/m$^2$ neutron flux to the tungsten first wall, volumetric heat deposition is about 45 W/cc, equivalent to about 0.45 MW/m$^2$ for the 1 cm thick tungsten plate.

Table 1 shows machine parameters of ITER-FEAT, DEMO reactors (designed by JAERI), and some commercial fusion reactor designs [7–10]. ITER-FEAT will be the first long-pulsed burning plasma device and its impacts on plasma physics and fusion technology are very large. But to look ahead to DEMO and the following commercial reactors, significant progress is still needed. Since the fusion power will increase roughly by an order of magnitude going from ITER-FEAT to DEMO and future commercial reactors without significant change in machine size (except SEAFP), resulting significant increase in neutron flux and heat flux along with higher duty cycle represent challenging tasks for blankets (and for divertors).

### 2.2. Fast neutral and ion fluxes

Fast neutrals of deuterium and tritium produced in plasma edge through charge-exchange (CX) reactions can play a dominant role on erosion in first wall materials. Plasma ions including deuterons and tritons as well as helium ions and impurity ions in scrape-off layer (SOL) also impinge on the wall but their fluxes are lower than that of DT CX flux. In ASDEX-U, characteristics of CX flux to the first wall and its effect on erosion were estimated by using B2/EIRENE simulation [11]. This work showed that particle flux and its mean energy had a strong effect on the wall erosion. In ITER-FEAT, particle flux at the first wall of blankets and its mean energy were estimated [1,12]. Localized gas puffing and resultant recycling at the top of the chamber produce the largest flux ($\sim 10^{21}$ m$^{-2}$ s$^{-1}$) and the lowest mean energy ($\sim$6 eV). At this flux peak, erosion of beryllium and tungsten takes local minimum due to very low mean energy. The peak erosion of beryllium and tungsten takes place aside from the gas puffing position. The beryllium peak erosion rate is $\sim$3.5 mm/yr and tungsten erosion is between one and two orders of magnitude lower.

For DEMO and future commercial reactors, core plasma parameters would significantly change in comparison with ITER-FEAT. The average plasma density increases by a factor of roughly 2 compared with ITER-FEAT and then density in the SOL may be increased. In addition, it was reported by LaBombard et al. [13] that an effective diffusivity and associated fluctuation levels became large across the entire SOL and cross-field heat convection exceeds parallel conduction losses as the discharge density limit is approached. This phenomenon impacts heat and ion fluxes to the first wall in high density plasmas. Particle control in the divertor also affects SOL plasma property. Mahdavi et al. reported that diverter pumping reduced the SOL density far upstream from the divertor and the $D$ line intensity in DIII-D [14]. They also showed that divertor pumping reduced the wall particle inventory. These results suggest that the particle flux to the first wall decreased by divertor pumping. Increase in the SOL density reduces the mean free path of neutrals recycled from the first wall as well as CX neutrals produced in the plasma. Therefore, CX neutrals produced only near the surface of the SOL can impinge onto the first wall and the mean energy of CX neutrals can be reduced. On the other hand, increase in edge density can increase ion flux to the wall.

Advanced plasma operation modes such as a reversed shear mode with pedestal near the plasma edge, where steep temperature and density gradient near the separatrix exists, would also affects the characteristics of CX neutrals to the first wall. In this case, high temperature region exists near the separatrix and fast neutrals produced in this region can have high particle energy, which may escape from the plasma and cause high erosion rate of the first wall.

As mentioned above, CX flux is higher near the gas puffing location due to high neutral density. This

Table 1
Machine parameters of fusion reactors

| | ITER-FEA-TExp. reactor | SSTR Demo | DEMO (JAERI) | SEAFP Comm | A-SSTR2 Comm | CREST Comm | ARIES-RS Comm |
|---|---|---|---|---|---|---|---|
| $R$ (m) | 6.2 | 7 | 5.8 | 9.5 | 6.2 | 5.4 | 5.52 |
| $a$ (m) | 2 | 1.75 | 1.45 | 2.09 | 1.5 | 1.59 | 1.38 |
| $I_p$ (MA) | 15 | 12 | 12 | 10.4 | 12 | 12 | 11.3 |
| $B_t$ (T) on-axis | 5.3 | 9 | 9.5 | 7.8 | 11 | 5.6 | 8.0 |
| $B_t$ (T) max | 12 | 16.5 | 20 | 12.8 | 23 | 12.5 | 15.8 |
| $T_e$ (keV) | 9.8 | 17 | 18 | 10 | 19 | 15.4 | 18.7 |
| $\langle n_e \rangle$ ($10^{20}$ m$^{-3}$) | 1.04 | 1.4 | 1.94 | 1.62 | 2.7 | 2.1 | 2.11 |
| $\beta_N$ (%) | 1.9 | 3.5 | 4 | 3.5 | 4.2 | 5.5 | 4.8 |
| $P_{fus}$ (GW) | 0.5 | 3 | 2.3 | 3.0 | 4.0 | 2.97 | 2.17 |
| $N_{load}$ (MW/m$^2$) | 0.57 (ave) | | 3 (ave) | 2.1 (ave) | 6 (ave) | 4.5 (ave) | 4.0 (ave) |
| | 0.78 (max) | 3 (max) | 5 (max) | | 8 (max) | 6.5 (max) | 5.7 (max) |
| Heat load [FW] (MW/m$^2$) | 0.25 (ave) | | 0.5 (ave) | 0.4 (ave) | 1.0 (ave) | 1.2 (ave) | |
| | 0.5 (max) | 1 (max) | 1.0 (max) | | | | 0.4 (max) |
| Heat load [DV] (MW/m$^2$) | 10 | 7 | 10 | | 4 | 10 | 6 |

indicates that fueling and neutral density are closely related. In future reactors, pellet injection can be an indispensable fueling method in order to increase fueling efficiency. For pellet injection, neutral density near the plasma edge is reduced, while neutral density in the inner hotter region is increased. Therefore, mean energy of CX neutrals can be increased but its flux to the wall can be decreased due to re-ionization of CX neutrals in edge plasma.

### 2.3. Energetic particle loss

The presence of energetic particles, specifically 3.5 MeV alpha particles, is one of the key differences between present day devices and burning plasma devices. Some of alpha particles escape from the core plasma and impinge on the first wall before thermalization. A key mechanism of this energetic ion loss has been known as ripple transport, caused by toroidal field (TF) ripple due to discreteness of toroidal field coils. The effects of TF ripple on the confinement of energetic particles in tokamaks have been well studied both theoretically and experimentally [15]. Numerical results were validated by comparison with experimental results (neutron decay following neutral beam pulse injection, the loss-related heat load on the first wall [16], trapped alpha distribution function by pellet charge exchange diagnostics [17] and deposition distribution measurements of energetic tritons on the armor tiles by a tritium imaging technique [18,19]).

Ripple loss has strong dependence on TF ripple amplitude and safety factor $q$. TF ripple amplitude $\delta$ is defined as $(B_{max} - B_{min})/(B_{max} + B_{min})$, where $B_{max}$ and $B_{min}$ are the maximum and minimum toroidal field. Since high $q$ leads to an increase in the ripple loss [20] due to a weak poloidal field in the core plasma, reversed shear operation with high $q$ (in particular, high $q$-minimum) would be a critical issue in the tokamak reactor operation. According to ripple loss estimation for ITER-FEAT by an orbit following Monte Carlo (OFMC) code [21,22], the power deposition of alpha particles on the wall is 6.8% of the generated alpha particle power of ITER-FEAT (100 MW) and the resulting heat flux is 0.8 MW/m$^2$ at the peak. In this calculation, $q_{min} = 2$ (reversed shear mode) and uniform alpha particle production were assumed. The total heat flux (radiation $\sim 0.3$ MW/m$^2$ and alpha particle loss 0.8 MW/m$^2$) would be $\sim$1.1 MW/m$^2$, which is unacceptable for the ITER-FEAT first wall. Fig. 1 shows energy distribution of the incoming alpha particles to the wall [21]. A prompt alpha particle loss produced in the peripheral region of the plasma is responsible for a sharp peak near the birth

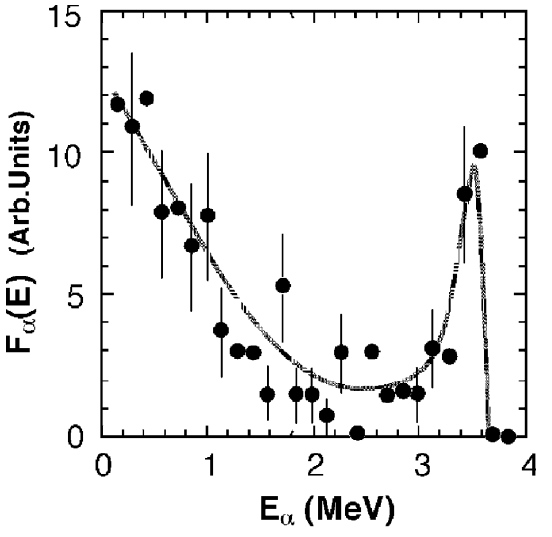


Fig. 1. Energy distribution of ripple loss alpha particles for $q_{min} = 2$, flat $S_\alpha$, and no TF ripple reduction [21].

energy (3.5 MeV), which is reduced when the birth profile of alpha particles is peaked or when TF ripple is lowered.

Ideas of reduction of TF ripple by ferromagnetic inserts (FI) were proposed by several groups [23,24]. JAERI first demonstrated its effectiveness in JFT-2M [25]. In ITER-FEAT without FI, the maximum TF ripple amplitude at the separatrix $\delta$ is $\sim$1.1%. According to calculations carried at JAERI [22], by optimizing the fraction of FI in the in-wall shielding for ITER-FEAT, TF ripple can be sufficiently reduced. The ripple loss of 6.8% without FI is reduced to 0.4% with optimized FI, see Fig. 2. The resulting alpha particle heat load is $<0.1$ MW/m$^2$ for ITER-FEAT. If this ripple loss rate holds for the power reactor with the fusion output of 2 GW, the resulting ripple loss power is $<0.4$ MW/m$^2$, corresponding alpha particle flux of $<2\times10^{18}$ m$^{-2}$ s$^{-1}$. According to Behrisch et al. [12], this flux is comparable to thermal He ion flux. The production of energetic triton and proton generated by *D–D* fusion reaction is two orders of magnitude lower. They deposit in the same area as the alpha particles. The ripple loss is mainly caused by trapping of energetic particle with very low parallel velocity in TF ripple and drifting across the magnetic field until they exit the plasma and strike the wall. Therefore, the location of deposition is strongly dependent on TF ripple structure. This is the reason why different energetic particles deposit in the same area.

Ripple losses of energetic particles affect surface modification of the first wall. These issues will be discussed in Section 4.

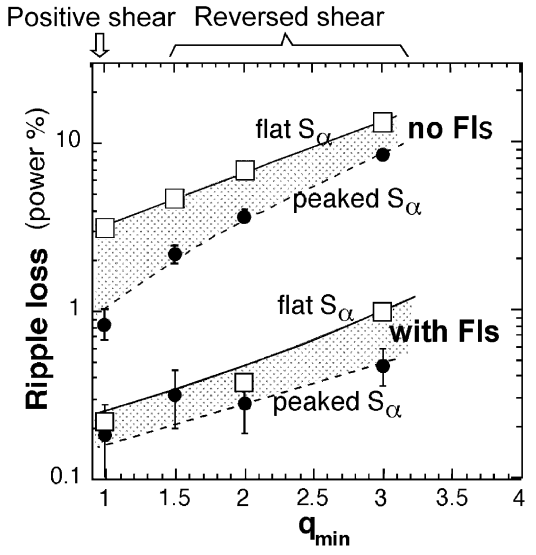


Fig. 2. Alpha particle ripple losses vs. minimum $q$ without TF ripple reduction (no FIs) and with TF ripple reduction. $S_\alpha$ denotes alpha particle production profiles [22].

## 3. Blanket first wall design and its effect on blanket functions

### *3.1. Blanket system and characteristics of low activation materials for first wall*

Table 2 shows typical blanket concepts for DEMO and commercial reactors [10,26–31]. All systems in Table 2 employ low activation structural materials such as RAF (reduced-activation ferritic/martensitic steel), vanadium alloys (e.g. V–4Cr–4Ti), and $SiC_f$/SiC composites. In most of these concepts, plasma facing first-walls were made by structural materials itself, because armor materials such as W could bring another issues (e.g. stress due to different thermal expansion between armor and wall materials, reduction of TBR, and an increase in radioactive dust).

It must be noted that first-wall thicknesses for all designs are relatively thin (a few mm) regardless of materials. The major engineering constraints determining first-wall thickness are stress (primary and secondary (thermal)) and temperature limit of the materials. As the first wall thickness increases, thermal stress increases in proportion to thickness. Then there exists maximum allowable thickness, which is in mm range in the first wall environments. In order to make the detailed stress calculation in the first walls, the geometrical parameters of the blanket and coolant pressure have to be also taken into consideration.

Thermal characters of these materials are briefly summarized in Table 3 [32,33]. Figure of merit for surface heat capability can be estimated with the value of $M$, which is defined as follows [33]:

$$M = 3S_m\kappa(1-\nu)/(\alpha_i E). \quad (1)$$

Here, $S_m$ is the allowable primary membrane stress intensity, $\kappa$ is thermal conductivity, $\nu$ is Poisson's ratio, $\alpha_i$ is the coefficient of linear thermal expansion, and $E$ is the Young's modulus. The value of $M$ approximately corresponds to the product of the maximum allowable heat flux and wall thickness. In order to handle high heat fluxes from core plasmas, relatively thin first walls must be used. These requirements conflict with the need to have longer first-wall lifetime against erosion.

For DEMO blanket designs, RAF is mainly employed because of its maturity in terms of a developed technology and a broad industrial experience. It also shows reasonably good thermophysical and thermomechanical properties. However, its temperature limit ($\sim$550 °C) does not allow for high coolant temperature, resulting in moderate power conversion efficiency (up to $\sim$40%). The surface temperature limit could be increased by using oxide dispersion-strengthened (ODS) grades at the surface, where the high temperature zones are localized.

Table 2
Blanket systems

| | He cooled pebble bed | Water cooled pebble bed | Water cooled Pb-17Li | Self-cooled flibe | Self-cooled Li | He cooled Li | Self-cooled Pb17Li (TAURO) | He cooled pebble bed (advanced) |
|---|---|---|---|---|---|---|---|---|
| Device | Tokamak DEMO | Tokamak DEMO | Tokamak DEMO | Helical FFHR-2 | Tokamak | Tokamak LAR design | Tokamak SEAFP | Tokamak |
| Structural material | ODS steel RAF | F82H, ODS RAF | EURO-FER RAF | V-Alloy | V-Alloy | V-Alloy (W coating) | $SiC_f/SiC$ | $SiC_f/SiC$ |
| Fusion power (GW) | 3.6 | 2.3 | 3.6 | 1.0 | | 5.3 | 3.0 | 4.5 |
| Neutron load ($MW/m^2$) | 4.4 (max) | 5.0 (max) | 6.6 (max) | 1.7 (ave) | 10 (max) | 11 (max) | 2 | 3.5 (max) |
| Surface heat load ($MW/m^2$) | 0.8 (max) | 1.0 (max) | 1.2 (max) | 0.1 (ave) | 2 (max) | 2.73 (max) | 0.5 | 0.6 (max) |
| FW thickness (mm) | 5 | 3 | 4 | 5 | 4 | 1.5 + 1(W), tubing | 3 | 3 |
| FW temperature (°C) | 630 | ~600 | 590 | 750 | 754 | 697 | <1300 | 913 |
| Coolant | He | $H_2O$ | $H_2O$ | Flibe | Liq. Li | He | Pb–17Li | He |
| Pressure | 8 Mpa | 25MPa | 15.5 MPa | 0.6 Mpa | 0.5 MPa | 15 MPa | 1.5 MPa | 8 MPa |
| Tritium breeder | Li Ceramics | $Li_2TiO_3$ | Pb–17Li | Flibe | Li | Li | Pb–17Li | $Li_4SiO_4$ |
| Neutron multiplier | Be | Be ($Be_{12}Ti$) | None | Be | Be | None | None | Be |
| Reference | [27] | [10] | [27] | [30] | [28] | [31] | [29] | [26] |

Table 3
Low activation material properties

| | RAF (F82H) | V-Alloy (V4Cr4Ti) | $SiC_f/SiC$ (see comment)[a] | W-Alloy |
|---|---|---|---|---|
| Surface heat capability $M$ (KW/Km) (temperature) | 3.1 (550 °C) | 4.6 (700 °C) | 1.1 (1000 °C) | 4–8 (1100 °C) |
| Thermal conductivity $\kappa$ (W/mK) (temperature) | 32 (550 °C) | 34 (700 °C) | 12.5 (1000 °C) | 85 (1100 °C) |
| Young's modulus $E$ (GPa) (temperature) | 184 (550 °C) | 121 (700 °C) | ~400 (1000 °C) | |
| Linear thermal expansion $\alpha_i$ ($10^{-6}$ $K^{-1}$) (temperature) | 12.3 (550 °C) | 11.4 (700 °C) | ~2.5 (1000 °C) | |
| Operating temperature (°C) | ~550 | | | |
| Upper limit | ~700 (ODS) | ~700 | ~1100 | ~1200 |
| Lower limit | ~300 | ~400 | ~600 | ~900 |

Definition of surface heat capability $M$ was expressed in Eq. (1). Data in this table are cited from Ref. [33].
[a] These $SiC_f/SiC$ data are based on Ref. [32], where neutron-irradiation data to CVI $SiC_f/SiC$ are shown.

In order to construct more economical reactors with high conversion efficiency (>45%), V-alloy and $SiC_f/SiC$ composite would be employed. Especially, by using $SiC_f/SiC$, whose operating temperature would be 1100 °C [34], power conversion efficiency more than 50% could be obtained. For blanket designs with V-alloy, acceptable neutron and surface heat load exceed 10 $MW/m^2$ and 2 $MW/m^2$, respectively. When they are reduced to 3.4 and 0.7 $MW/m^2$, the thickness of the V-alloy wall can be increased to ~12 mm in the case that the highest temperature is ~690 °C [35]. Because of its excellent surface heat capability and low activation, V-alloys are very attractive. But, environmental impurity effect (oxygen etc.) on V-alloy is a matter of concern. For example, oxidation of V-ally can deteriorate its mechanical property even with 300 ppm oxygen [36]. From this viewpoint, surface coatings on the plasma facing side would be needed as diffusion barrier of hydrogen isotope and impurities, even if sputtering erosion is negligible.

In terms of surface heat capability, $SiC_f/SiC$ composite made by a chemical vapor infiltrated (CVI) method is not as good as V-alloy mainly due to low thermal conductivity, which leads to lower acceptable

surface heat load than V-alloy. In view of very recent $SiC_f/SiC$ composite development [37], however, surface heat capability for $SiC_f/SiC$ composite is significantly improved and can exceed RAF and V-alloy. Therefore, blanket designs with high temperature operation and high surface heat capability may be realized with newly developed $SiC_f/SiC$ composite.

### 3.2. Effects of first wall materials on TBR

Blankets have an important function such as breeding tritium with TBR of more than about 1. The supply of tritium will determine the speed of introduction of the commercial plant. In order to achieve a satisfactory introduction speed of fusion reactors, the early phase plants must produce initial inventory for subsequent reactors in a reasonably short time. For this purpose, total TBR needs to be at least 1.07 [38]. Most of present blanket designs fulfill this requirement, but the margin of TBR is usually very small. Therefore, any effect potentially reducing TBR must be considered seriously.

For the protection against erosion, tungsten is one of the best candidates for the armor material because of its low erosion yield. In terms of neutronics, tungsten has two different characters. One is very high $(n, 2n)$ cross section ($\sim$2 barns at $\sim$14 MeV). The other is very high neutron capture cross section especially below several hundreds keV. Therefore, for about 14 MeV neutrons, multiplication of neutron takes place, but for backscattered neutrons with energy significantly reduced, the tungsten first-wall will capture neutrons, leading to deterioration of the breeding function. To better quantify these effects and the resulting impact on TBR, detailed neutronics calculations and system optimization are required.

The effects of tungsten first-wall and armor on TBR were examined for water-cooled DEMO blankets [39] and for advanced blankets [40,41]. For the water cooled ceramic breeder blanket for DEMO, Sato et al. made detailed calculation about the effect of first-wall materials and its thickness on TBR [39]. In this blanket system, the structural material and the coolant are F82H and water. Using Be as an armor, the TBR increases with armor thickness. Instead, TBR decreases using a W armor. This TBR reduction for W, however, can be mitigated by putting a breeding layer ($LiO_2$) just behind the first wall (F82H with water coolant channel) and by enrichment of $^6$Li. Fig. 3 shows the TBR as a function of W armor thickness for two configurations. For case I the breeder layer of 7.1 mm is arranged just behind the first wall (first layer), while for case II multiplier layer (Be) of 24.1 mm is the first layer. It is clearly observed that TBR reduction is not large for case I with 30% $^6$Li. By employing this configuration, the effect of neutron capture by the W armor on TBR reduction can be mitigated.

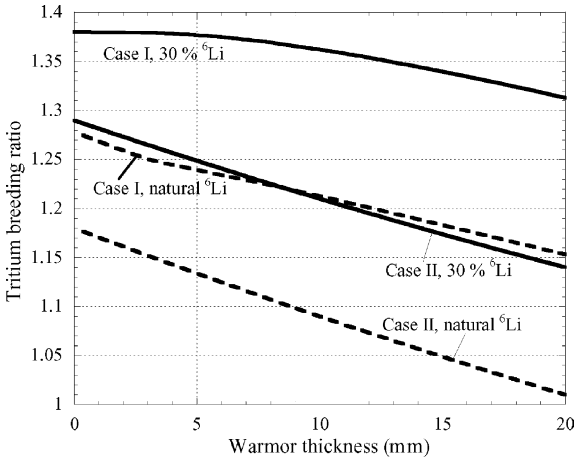


Fig. 3. TBR vs. W armor thickness. For case I breeding layer ($Li_2O$) is the first layer, while for case II multiplier layer (Be) is the first layer [39].

## 4. Erosion and surface modification of first wall materials

### 4.1. Sputtering erosion

In Fig. 4, physical sputtering yields of three low activation materials together with Be and W are shown. In these data, sputtering yields were calculated by using revised Bohdansky formula [42]. For Be erosion, the work by Roth et al. [43] are referred. For SiC, the yield data in Ref. [44] was used. Here, yields data of V-alloy and RAF are substituted for V and Fe data, respectively.

The sputtering yields of RAF, V-Alloy, and SiC are similar. Differences of the yields are less than a factor of two excluding the yields near threshold energies. Compared with Be, these yields are lower by a factor of 3–5 at the energy of 100 eV. Difference of the yields becomes

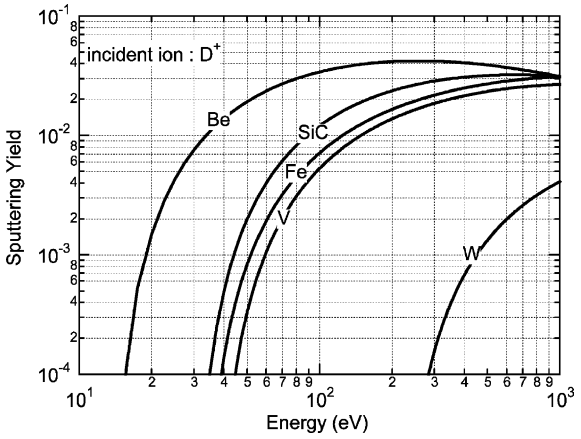


Fig. 4. Energy dependence of physical sputtering yields by $D^+$ for Be, SiC, Fe (RAF), V (V-Alloy), and W.

smaller with increasing energy. For SiC, chemical sputtering in the energy less than 100 eV could enhance the yield [45]. According to the ITER-FEAT estimation made by Behrisch et al. [12], erosion rate of Be (~3.5 mm/yr) and Fe (~2 mm/yr) are not very different. By considering the first wall thickness shown in Table 2 (3–5 mm) and a blanket replacement period of about 3 years, these erosion rates are beyond the acceptable level.

For especially high $Z$ material erosion, effect of volatile impurity ions such as oxygen and inert gases for divertor plasma cooling can play an important role because they have much lower threshold energy for high $Z$ material sputtering than hydrogen isotopes. If non-volatile materials (e.g. carbon) exist in the plasma, erosion behavior changes with impurity ion concentration. There is a critical concentration, beyond which non-volatile materials accumulate on the wall and protect it against erosion [46]. When significant part of the walls are covered by tungsten and the self-sputtering yield exceeds 1, runaway sputtering of W would occur, which must be avoided. Considering angular distribution and sheath acceleration, the condition of the unity yield is realized in the edge electron temperature of ~35 eV for $W^{6+}$ [47].

### 4.2. Blistering

Light ions (helium and hydrogen isotopes) impinging on metallic materials and $SiC_f$/SiC composites (helium) cause blistering [48,49], when they are subjected to high fluence of incident ions. The critical helium fluence, at which blisters start to appear, has been found experimentally to be in the range from $10^{21}$ to $10^{22}$ He/m$^2$. Thickness of blister skins and size of blisters increase with energy. At the He energy of 3.0 MeV, the critical fluence for W is about $0.5 \times 10^{22}$ He/m$^2$ with average blister diameter of about 130 μm [50].

Hydrogen isotopes also cause blistering on metallic materials [51–54], but its characters are different from those of helium. The critical fluence of deuterium blistering for tungsten is in the range from $10^{23}$ to $10^{24}$ D/m$^2$ [52,53], about two orders of magnitude higher than helium. Hydrogen blistering occurs in the temperature ranges $\lesssim$ 600 °C [53,55] for tungsten and $\lesssim$ 300 °C for molybdenum [51]. On the other hand, helium blistering are observed even at about half of the melting point (about 1450 K) for molybdenum [48]. The reason is attributed to high binding energy of helium atoms to the defects compared with hydrogen isotopes.

The important issues concerning blistering are its effect on erosion enhancement together with dust formation. Due to the formation of blisters, first wall materials can be released into the plasma by flaking, grain ejection, or evaporation of thin blister caps. It was reported that surface roughness and energy distribution of incident ions could mitigate or suppress the blister formation [48,53]. But in actual fusion reactor environments, such as high particle fluence and high heat load as well as high neutron load, their effects on blister formation and related erosion are not known.

On the locations where alpha particles due to ripple loss (flux of about $10^{18}$ He/m$^2$ s) impinge, large helium blisters could be formed on metallic materials and $SiC_f$/SiC composites in the fluence more than about $10^{22}$ He/m$^2$ (reached within only one day operation) even under high blanket surface temperature conditions (roughly 500–1000 °C), where hydrogen blistering can not appear. Therefore, the effect of blistering on erosion enhancement due to alpha particle ripple loss could be an important issue for the blanket first wall.

Mixing of plasma facing materials can significantly complicate plasma surface interaction in terms of not only erosion but also blistering. Recently, the effect of carbon impurity with less than 1% on enhancement of hydrogen blister formation on tungsten was investigated with hydrogen and carbon mixed ion beam irradiation [54,55]. The reason for this phenomenon could be attributed that carbon contained layer near the surface controls hydrogen diffusion into the bulk and enhances blister formation.

### 4.3. Helium embrittlement and codeposition issues

In general, the accumulation of helium in metallic materials, especially for high $Z$ materials such as molybdenum and tungsten, is much more harmful than hydrogen because its strong interaction with defects [56]. Helium enhances the formation of bubbles, leading to local swelling and degradation of mechanical properties of bulk materials. It was claimed that helium irradiation embrittlement took place not only at room temperature but also at 973 K [56]. Therefore, especially at the impinged location of alpha particle ripple loss, much attention has to be paid to such degradation of mechanical properties. Synergistic effects with neutron irradiation could also be important.

In terms of in-vessel tritium retention, codeposition of tritium with eroded wall materials is a matter of concern, especially when graphite divertor plates are used for ITER-FEAT [1]. For DEMO and future reactors, selection of first-wall materials also needs this point of view. Codeposition of pure metallic materials with the tritium could not be a serious problem. But the effect of small amount of impurity such as oxygen on tritium retention is a point to notice. It was shown that hydrogen retention significantly increased in the Mo codeposition layer containing oxygen [57,58]. They implanted 6 keV $D_3^+$ ion beam at the fluence of $3 \times 10^{21}$ D/m$^2$ at RT into Mo-deposition layer deposited in oxygen atmosphere from RT to 773 K. For the Mo-deposition layers formed at RT, 31% of implanted deuterium was retained, while for those formed more

than 573 K deuterium retention was negligible. On the other hand, when $SiC_f/SiC$ composite is used for the plasma facing surface, codeposition issue could become an important issue. The mixed layer of Si and C can contain up to 0.7 D/(Si + C), which does not decrease significantly until about 600 K [59].

### 4.4. First wall material options

If low activation structural materials can be used as plasma facing surfaces of blankets, it is very preferable in terms of simplicity of blanket system. But sputtering erosion due to CX neutrals and plasma ions would not be tolerable, if erosion of the first walls for DEMO and future reactors are similar to or more than those of ITER-FEAT. In addition, aside from erosion issues, H/He embrittlement along with neutron effects is an important issue to be considered. If erosion or other degradation of low activation materials as first walls is not acceptable, armor materials with low erosion yield such as W or some protection methods such as low $Z$ in-situ coating would be needed. Since tungsten has very low erosion and relatively low activation (but not negligible), it is one of the strongest candidates for armor materials. Development of reliable coating methods to the first wall and evaluation of H/He blistering and embrittlement, which might enhance effective erosion, and optimization of blanket system in terms of TBR are important issues.

For low $Z$ material coating such as Be and B, developments of in-situ and very rapid coating methods are necessary due to high erosion rate. Beryllium has many preferable aspects, other than low $Z$ and oxygen gettering ability, such that TBR could be increased with Be coating and its effect on tritium codeposition could be small. Its safety issues due to toxicity, however, might offset these advantages. Boron is another candidate with similar advantages to Be in terms of low $Z$ and oxygen gettering. Its principal issue is to form thick (in mm range) adherent films on the first wall. In addition, since $^{10}B$ has very high neutron absorption cross section, isotope separation to leave only $^{11}B$ must be done.

## 5. Effects of first wall on core plasma performance

### 5.1. Hydrogen recycling

The highest plasma confinement and DD neutron production in present day tokamaks have been obtained in low-density discharges under the low recycling conditions such as reversed shear mode, supershot, and hot ion H mode [60–62]. All these regimes need wall conditioning procedures in order to reduce recycling. Low recycling wall conditions are also needed to obtain reproducible startup conditions and a good plasma current rampup. In steady-state reactors, however, the effect of conditioning does not last long and recycling rate of the first walls soon becomes approximately 1.0, which brings the issue of production and sustainment of high performance core plasmas under the high recycling condition.

In TRIAM-1M, in ultra-long discharge, the recycling coefficient $R$ showed fluctuation around 1.0; sometimes $R$ exceeded 1.0 (releasing gas) and then $R$ decreased below 1.0 (absorbing gas), i.e. the wall repeated processes of saturation and refreshment [63]. The reason could be attributed to deposition of wall materials, which created new unsaturated surface. For steady-state reactors, it can be speculated that once the high performance plasma is achieved, neutral recycling flux from the first wall does not affect the plasma performance very much because of high density SOL plasma and short penetration length of neutrals toward the core plasma. Even in this case, enough pumping performance is needed to suppress the effect of the over-recycling ($R > 1$) in a steady-state operation.

### 5.2. Reflection of synchrotron radiation

In future fusion reactors, the synchrotron radiation loss plays an important role in the power balance of the fusion plasma. For tokamak fusion reactors with a high magnetic field (about 10 T or more), synchrotron radiation is the order of 50 MW. The net value of synchrotron radiation loss is proportional to $(1-R)^{1/2}$ where the $R$ denotes power reflectivity of the first wall. Therefore, the choice of the first wall materials can affect the energy confinement through the reflection of the synchrotron radiation. For example, for the DEMO plant planned in JAERI, the $H_H$ factor [64] of 1.8 is necessary for $R = 0$ according to a 0-D system code analysis, but for $R = 1.0$ it decreases to 1.5.

According to Takeda et al. [65], tungsten and graphite with high electrical conductivity $\sigma_e$ have high reflectivity of about 0.9 to 1.0, while the reflectivity of SiC is low (about 0.3). Therefore, using the metallic first wall (high electrical conductivity) would be preferable in terms of effective use of synchrotron radiation. Nagatsu, however, also showed that ion-beam irradiation (50 eV H) up to the fluence of about $10^{24}$ $m^{-2}$ tended to decrease the reflectivity of CFC (graphite) [66]. This reflectivity degradation could be recovered by Be coating.

## 6. Conclusions

Issues for the first wall of blankets are summarized below.

1. Reliable estimation of flux and energy of fast neutrals, plasma ions (fuel ions, impurity ions from the wall and for radiative cooling, and He ash), and energetic

alpha particles onto the first walls by considering the following effects:

- Confinement modes (especially with pedestal).
- Fueling methods (Gas puffing and pellet injection).
- Anomalous cross field transport near the density limit.
- Particle control (pumping and gas puffing) in the divertor.
- Impurity gas injection for radiative cooling.
- Toroidal field ripple for energetic alpha particle loss.

2. Feasibility assessment for low activation materials as the plasma facing surface in terms of erosion and material degradation by physical and chemical (for $SiC_f$/SiC composite) sputtering, blistering, embrittlement by hydrogen isotope and helium ions implanted from the plasma facing surface, and in terms of effects of eroded atoms and flakes on plasma performance and safety (codeposition with tritium and dust). Synergistic effects of neutron irradiation and material mixing effects need to be considered.
3. Assessments of surface protective armors and coatings from the same viewpoints shown above and, in addition, in terms of coating methods (in-situ coating is necessary especially for low $Z$ materials such as B and Be) in the case that bare surfaces of low activation materials are inappropriate due to mainly erosion and material degradation.
4. Optimization of blanket structures considering the first wall materials (especially for W) in terms of TBR.
5. Evaluation of the effect of high recycling first walls on core plasma performance and optimization of plasma control methods.
6. Evaluation and optimization of reflectivity of synchrotron radiation especially after high fluence particle load and in-situ coating.

## Acknowledgements

The authors are deeply grateful to many researchers in Japan, USA, and Germany for fruitful discussions, variable comments, and providing important data.

## References

[1] G. Federici et al., J. Nucl. Mater. 290–293 (2001) 260.
[2] M.A. Abdou, The APEX Team, Fus. Eng. Des. 54 (2001) 181.
[3] R. Bastasz, W. Eckstein, J. Nucl. Mater. 290–293 (2001) 19.
[4] M. Ulrickson, ISFNT6 (2002), Fus. Eng. Des., in press.
[5] P. Wurz et al., J. Nucl. Mater. 290–293 (2001) 1138.
[6] ITER Physics Expert Groups on Divertor and Divertor Modelling and Database, Nucl. Fus. 39 (1999) 2391.
[7] I. Cook, Fus. Eng. Des. 25 (1994) 179.
[8] F. Najmabadi, The ARIES Team, Fus. Eng. Des. 38 (1997) 3.
[9] Y. Asaoka et al., Fus. Eng. Des. 48 (2000) 397.
[10] S. Konishi et al., ISFNT6 (2002), Fus. Eng. Des., in press.
[11] H. Verbeek et al., Nucl. Fus. 12 (1998) 1798.
[12] R. Behrisch et al., these Proceedings (2002). PII: S0022-3115(02)01580-5.
[13] B. LaBombard et al., Phys. Plasmas 8 (2001) 2107.
[14] M.A. Mahdavi et al., J. Nucl. Mater. 220–222 (1995) 13.
[15] ITER Physics Expert Groups on Energetic Particles, Heating and Current Drive, Nucl. Fus. 39 (1999) 2471.
[16] K. Tobita et al., Nucl. Fus. 35 (1995) 1585.
[17] H. Duong et al., Nucl. Fus. 37 (1997) 271.
[18] K. Miyasaka et al., J. Nucl. Mater. 290–293 (2001) 448.
[19] T. Tanabe et al., J. Plasma Fus. Res. 77 (2001) 1083.
[20] K. Tobita et al., Nucl. Fus. 37 (1997) 1583.
[21] K. Tobita et al., Fusion Eng. Des., submitted for publication.
[22] K. Tobita et al., Plasma Phys. Control., in press.
[23] M.V. Ricci, N. Mitchell, Proceedings of the 15th SOFT, Utrecht (1988) 1565.
[24] G.V. Sheffield, PPPL-2876 (1993).
[25] M. Sato et al., Fus. Eng. Des. 51–52 (2000) 1071.
[26] L.V. Bocaccini et al., Fus. Eng. Des. 49&50 (2000) 491.
[27] L. Giancarli et al., Fus. Eng. Des. 49&50 (2000) 445.
[28] Y. Gohar, S. Majumdar, D. Smith, Fus. Eng. Des. 49&50 (2000) 551.
[29] H. Golfier et al., Fus. Eng. Des. 49&50 (2000) 559.
[30] A. Sagara et al., Fus. Technol. 39 (2001) 753.
[31] C.P.C. Wong et al., Fus. Eng. Des. 48 (2000) 389.
[32] D.J. Senor et al., Fus. Technol. 30 (1996) 943.
[33] A. Tavassoli, J. Nucl. Mater. 302 (2002) 73.
[34] A.R. Raffray et al., Fus. Eng. Des. 55 (2001) 55.
[35] I.R. Kirillov, RF DEMO Team, Fus. Eng. Des. 49&50 (2000) 457.
[36] T. Muroga et al, J. Nucl. Mater., in press.
[37] Y. Katoh et al., Ceramic Eng. Sci. Proc., in press.
[38] Y. Asaoka et al., Fus. Eng. Des. 30 (1996) 853.
[39] S. Sato, T. Nishitani, these Proceedings. PII: S0022-3115(02)01587-8.
[40] A. Sagara et al., Fus. Eng. Des. 41 (1998) 349.
[41] M.Z. Youssef, C. Wong, Fus. Eng. Des. 49&50 (2000) 727.
[42] C. Garcia-Rosales, W. Eckstein, J. Roth, J. Nucl. Mater. 218 (1994) 8.
[43] J. Roth, W. Eckstein, M. Guseva, Fus. Eng. Des. 37 (1997) 465.
[44] H. Plank, R. Schworer, J. Roth, Nucl. Instrum. and Meth. B 111 (1996) 63.
[45] M. Balden, S. Picarle, J. Roth, J. Nucl. Mater. 290–293 (2001) 47.
[46] D. Naujoks, W. Eckstein, J. Nucl. Mater. 220–222 (1995) 993.
[47] D. Naujoks et al., Nucl. Fus. 36 (1996) 671.
[48] G.M. McCracken, P.E. Stott, Nucl. Fus. 19 (1979) 889.
[49] S.K. Das, M. Kaminsky, Adv. Chem. Ser. 158 (1976) 112.
[50] B. Constantinescu, C. Sarbu, Fus. Eng. Des. 49&50 (2000) 171.

[51] Y. Nakamura, T. Shibata, M. Tanaka, J. Nucl. Mater. 68 (1977) 253.
[52] A. Haasz, M. Poon, J.W. Davis, J. Nucl. Mater. 266–269 (1999) 520.
[53] W. Wang et al., J. Nucl. Mater. 299 (2001) 124.
[54] T. Shimada et al., J. Plasma Fus. Res. 78 (2002) 289.
[55] T. Shimada et al., these Proceedings. PII: S0022-3115(02)01447-2.
[56] N. Yoshida, J. Nucl. Mater. 266–269 (1999) 197.
[57] T. Hirai et al., J. Nucl. Mater. 283–287 (2000) 1177.
[58] M. Miyamoto et al., J. Nucl. Mater., in press. PII: S0022-3115(02)01352-1.
[59] M. Balden, M. Mayer, J. Roth, J. Nucl. Mater. 266–269 (1999) 440.
[60] J.D. Strachan et al., Phys. Rev. Lett. 58 (1987) 1004.
[61] E.A. Lazarus et al., Phys. Rev. Lett. 77 (1996) 2714.
[62] Y. Koide, JT-60 Team, Phys. Plasmas 4 (1997) 1623.
[63] M. Sakamoto et al., Nucl. Fus. 40 (2002) 165.
[64] ITER Physics Expert Groups on Confinement and Transport and Confinement Modelling and Database, Nucl. Fusion 39 (1999) 2175.
[65] N. Takeda, M. Nagatsu, M. Shimada, J. Appl. Phys. 34 (1995) L849.
[66] M. Nagatsu et al., J. Nucl. Mater. 241–243 (1997) 1180.